College of Pharmaceutical Science, Zhejiang University of Technology, Hangzhou, Zhejiang, PR China

Improvement of dissolution and tabletability of carbamazepine solid dispersions with high drug loading prepared by hot-melt extrusion

Zilin Feng, Mengting Li, Wenxi Wang*

Received January 16, 2019, accepted April 16, 2019

**Corresponding author: Wenxi Wang, College of Pharmaceutical Sciences, Zhejiang University of Technology, 18# Chaowang Road, Hangzhou, Zhejiang, PR China*
yjw@zjut.edu.cn

Pharmazie 74: 523-528 (2019) *doi: 10.1691/ph.2019.9008*

Solid dispersions (SDs) have made great progress in the improvement of dissolution for poorly soluble drugs, however the low drug loading still limits their wide application. In the present paper, high carbamazepine (CBZ) loaded SDs with excellent dissolution and tabletability were prepared and characterized. The CBZ SDs were prepared with Eudragit EPO as carrier by hot-melt extrusion (HME) in the drug: carrier ratio of 4:1. Powder X-ray diffraction, differential scanning calorimetry, fourier transform infrared spectroscopy and powder dissolution was carried out to characterize the SDs. The results showed that the crystalline form the polymorph of CBZ in SDs was transformed into form I from form III after extruded at 140 °C. Wettability and microstructure of CBZ SDs were improved by the HME process, which promoted the dissolution significantly. More than 85 % drug dissolved within 5 min from CBZ SDs with even only 20 % Eudragit EPO as carrier. CBZ SDs tablets were prepared by direct tableting with a universal material testing machine at various compaction pressures. Compactibility and tabletability were enhanced significantly by the HME process. All of these results showed the CBZ SDs prepared by HME with 80 % CBZ and 20 % Eudragit EPO could improve the dissolution and tabletability significantly.

1. Introduction

Solubility and dissolution rate are very important physicochemical properties of active pharmaceutical ingredients (API) because they are critical attributes of bioavailability. Poor aqueous solubility will limit the absorption of API from the gastrointestinal tract and subsequent pharmacological effects. The number of poorly soluble drug candidates has been dramatically increased with the application of high throughout screening and combinatorial chemistry (Kawabata et al. 2011; Medarević et al. 2015). So the improvement of solubility or dissolution properties of poorly soluble API is a challenging task in oral formulation development. Solid dispersions (SDs) are considered one of the most successful strategies to improve the dissolution profile of poorly soluble drugs (Vasconcelos et al. 2007; Vo et al. 2013).

SDs were first reported by Sekiguchi et al. (1964), then received much attention and have since been used in dozens of commercial products. SDs are defined as dispersions of one or more active ingredients in an inert carrier or matrix in the solid state. The API can be molecularly dispersed within the solid state matrix, as in the case of solid solutions, or exist in crystalline or amorphous state (Wang et al. 2018). In the help of carrier, the size of API in SDs is reduced, the wettability is improved and the amorphous state is easily obtained, so the dissolution rate of API is often enhanced (Pan-On et al. 2017; Dos Santos et al. 2017). However, to achieve dissolution promotion satisfactorily, a high content of carrier is often required (Alshahrani et al. 2015; Djuris et al. 2013; Ma et al. 2018). This is not a problem for low dose drugs which have strong pharmacological effect, but is often an embarrassment for the drug with single dose above 400 mg. So in the practical view, a high API/carrier ratio is one of the objectives of SDs development. In the present study, we developed carbamazepine (CBZ) SDs with high drug loading as 80 %, which still have dramatic dissolution improvement effects.

Various techniques have been developed to prepare SDs such as solvent evaporation (Al-Hamidi et al. 2010), fusion method (Alam et al. 2015; Ye et al. 2007), high-voltage electrostatic spinning (Verreck et al. 2003), spray drying or congealing (Chen et al. 2016; Edueng et al. 2017), supercritical fluid technique (Yin et al. 2015) and hot-melt extrusion (HME) (Kulkarni et al. 2017; Gupta et al. 2015; Bhardwaj et al. 2018). With the advantages of a solvent-free, continuous process and easy scale-up, HME has become the most popular preparation method for SDs in the past decades. Although the direct shaping of hot melt extrudates such as injection molding, calendering and pelletizing is available, the dissolution of API is often slow so that they rarely can disintegrate efficiently. So milling extrudates into powder and then tableted with other excipients is more often used for solubility enhancement (Treffer et al. 2013). Nowadays the interaction between excipients and API has been widely studied, while limited research has been conducted on how the physico-mechanical properties of extrudates affect drug product performance (Agrawal et al. 2013; Boersen et al. 2014; Dinunzio et al. 2012; Mohammed et al. 2012). The impact of the HME process on the compressibility of the powder is complicated and material dependent. Ndindayino et al. (2002) investigated the effect of HME process on direct compression properties of isomalt and found that the melt extruded isomalt prepared at 150 °C showed excellent tabletability due to the transformation into an amorphous form which possesses higher plastical deformation ability (Ndindayino et al. 2002). However, Grymonpre et al. (2016) demonstrated the HME to deteriorate the tableting behavior of PVA and PVA-sorbitol systems. Furthermore, Mohammed et al. (2012) found the extrusion process did not affect the tableting properties. These conflicting results suggest that the tabletability of hot melt extruded systems may not follow a general trend, but be dependent on the materials (Boersen et al. 2014). So another objective of the present study was to evaluate the compression properties of CBZ SDs with high drug loading prepared by HME.

2. Investigations, results and discussion

CBZ is a typical of BCS II drug with low solubility and high permeability (0.12 mg mL^{-1} and 4.3×10^{-4} cm s^{-1}, respectively) (Kovacević et al. 2009). Nowadays, CBZ SDs have been investi-

gated extensively and the dissolution of CBZ has been enhanced greatly (Alshahrani et al. 2015, Bhardwaj et al. 2018). However, all these reported SDs contained low drug loading. When drug loading increased, the dissolution rate decreased significantly. In the present study, a novel CBZ SDs with high drug loading was prepared and characterized.

2.1. CBZ SDs characterization

2.1.1. Powder X-ray diffractometry (PXRD) analysis

Four anhydrous crystalline forms of CBZ have been found: P-monoclinic (form III), triclinic (form I), trigonal (form II) and a C-monoclinic (form IV). Form III is the most stable polymorph and usually used in commercial pharmaceutical formulations. Grzesiak et al. (2003) found the four forms were similar in energy and would transform to form I upon heating. To identify the solid state of CBZ before and after HME, PXRD diffractograms of CBZ, Eudragit EPO, their physical mixture of Eudragit EPO and CBZ (PM) and CBZ SDs were determined and are shown in Fig. 1. CBZ powder showed characteristic crystalline peaks at 2θ= 15.3°, 15.7°, 17.0°, 19.4°, 27.5° (Fig. 1b), which were in accordance with the pattern of form III reported in the Cambridge Structural Database (CSD) and previous studies (Kobayashi et al. 2000; Sethia and Squillante 2004; Liu et al. 2012; Deng et al. 2017). The diffractograms of PM were similar to those of untreated CBZ, while the SDs showed a very different pattern. The SDs exhibited characteristic crystalline peaks at 2θ=6.1°, 7.9°, 9.3°, 12.2°, 19.8°, which were specific for form I, as reported in the CSD and the literature (Grzesiak et al. 2003; Kobayashi et al. 2000; Deng et al. 2017; Rustichelli et al. 2000; Patil et al. 2017). The results illustrated that, after extrusion with Eudragit EPO, the crystalline form of CBZ had been transformed from III to I, which is consistent with the results reported by Huang et al. (2016).

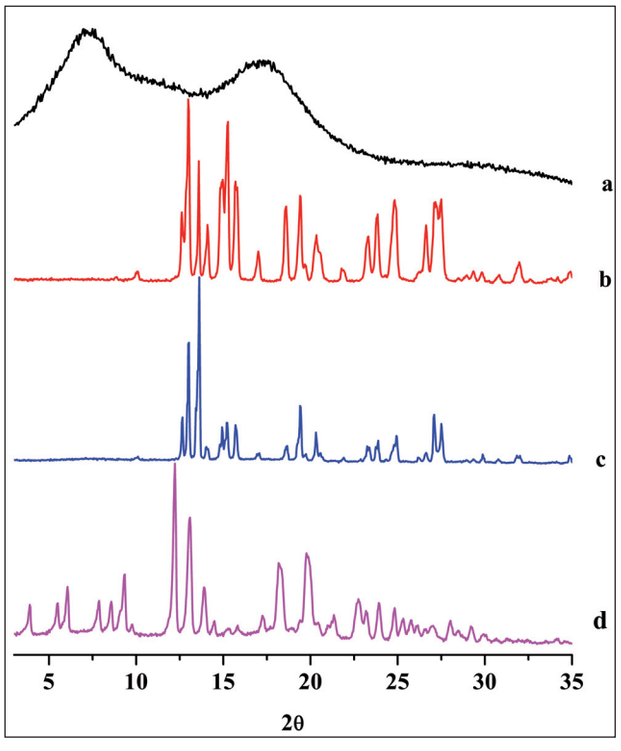

Fig. 1: PXRD patterns of EPO (a), CBZ (b), CBZ-EPO 4:1 PM (c),CBZ-EPO 4:1 SDs (d).

2.1.2. Differential scanning calorimetry (DSC) thermograms

The thermal behavior and crystalline phase transformation of CBZ, PM and CBZ SDs during the heating process were investigated by DSC and the thermograms are shown in Fig. 2. The DSC curve of CBZ powder as received showed the first endothermic peak at 175.7 °C, followed immediately by an exothermic peak and subsequently a sharp endothermic peak at 191.4 °C (Fig. 2a), which indicated the typical thermal behavior of form III with the melting of form III, crystallization of form I and melting of form I, respectively (solid-solid transformation of form III to form I). The sample of PM exhibited two endothermic peaks similar as pure drug with at 170.7 °C and 191.3 °C, respectively. However, for CBZ SDs, the DSC trace showed only one sharp endothermic peak around 190.0 °C. These results were in agreement with literature data (Grzesiak et al. 2003; Rustichelli et al. 2000) and indicated that CBZ may have been converted from form III to form I, which is consistent with the results of the PXRD.

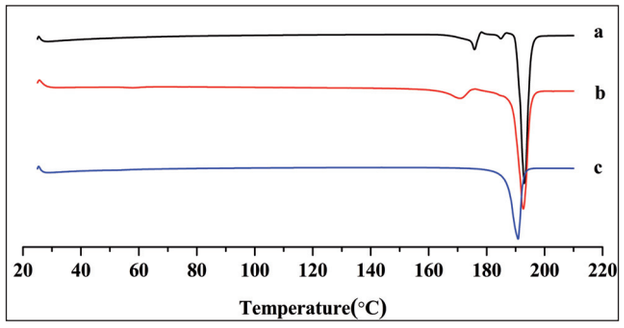

Fig. 2: DSC thermograms of CBZ (a), CBZ-EPO 4:1 PM (b), CBZ-EPO 4:1SDs (c).

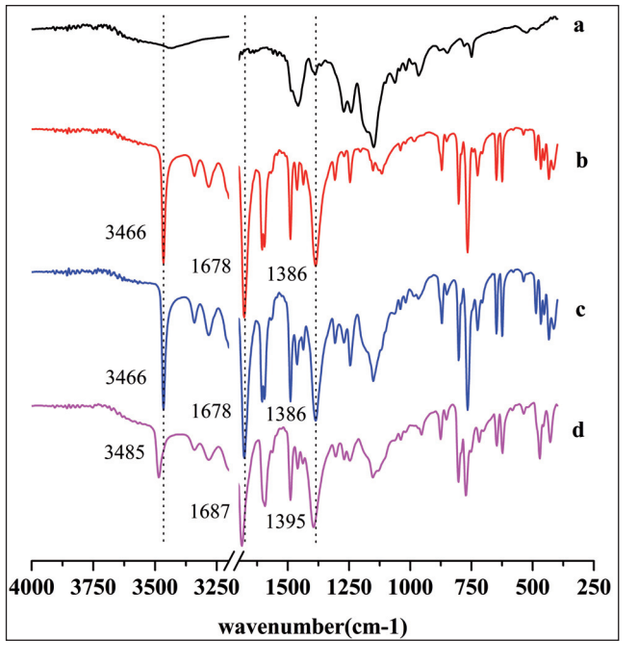

Fig. 3: FTIR spectra of EPO (a), CBZ (b), CBZ-EPO 4:1 PM (c), CBZ-EPO 4:1 SDs (d).

2.1.3. Fourier transform infrared (FTIR) spectroscopy

FTIR spectroscopy has been widely used to identify polymorphic forms. Differences in FT-IR spectra of CBZ forms that were crystallized under various procedures are known. Grzesiak et al. (2003) confirmed the existence of forms I and III by FTIR spectroscopy and provided some distinct differences between polymorphic forms and distinguished three ranges of wavenumbers, which seemed to be the most important for the differentiation (3500-3392 cm^{-1}, 1731-1629 cm^{-1}, 1427-1317 cm^{-1}).

FTIR spectra of CBZ, PM and CBZ SDs are illustrated in Fig. 3. The CBZ spectrum shows characteristic peaks at 3466 cm^{-1} (-NH valence vibration), 1678 cm^{-1} (-CO-R vibration), 1386 cm^{-1} (C-NH_2 stretching vibration) (Fig. 3b), which were corresponding

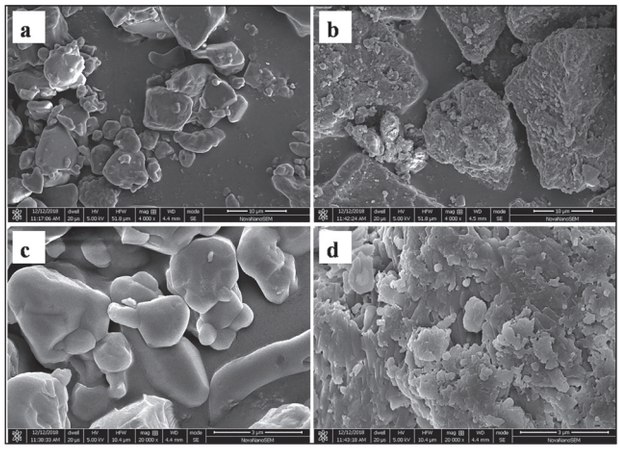

Fig. 4: SEM images of PM (a, c) and SDs (b,d) (a, b in 4000×magnification; c, d in 20000×magnification).

to those previously reported for polymorph III (Grzesiak et al. 2003; Douroumis et al. 2007). The PM presented similar peaks, suggesting that there was no intermolecular interaction between CBZ and the Eudragit EPO when only physically mixed together. However, obvious differences were observed in the spectra of SDs. The characteristic peaks marked by the dotted lines of SDs had all moved to higher wavenumbers: 3485 cm^{-1}, 1687 cm^{-1}, 1395 cm^{-1} (Fig. 3d), the characteristic peak of form I as reported in the literature (Grzesiak et al. 2003; Rustichelli et al. 2000). These results also confirmed that CBZ in SDs had been transformed to form I, which was in agreement with the PXRD and DSC results.

2.2. Scanning electron microscopy (SEM)

The microstructure of PM and CBZ SDs was observed by SEM (Fig. 4). It is obvious from the SEM images that the SDs showed very different morphologies compared to untreated PM. The images of PM showed a smooth particle surface, in which small spherical Eudragit EPO were attached to the surface of the large prismatic CBZ (Fig. 4 a, c), whereas the microscopic morphologies of SDs had changed a lot, which were rough and full of pores and voids (Fig. 4b). Further analyzing the SD particles at higher magnifications, the observation of the surface of the particles revealed that they were aggregated by many nanometer-sized strips (Fig. 4d). This indicated that after HME, CBZ was mainly present in the SDs in the form of nanometer-sized particles. Therefore, when the SDs contact the medium, the carrier dissolves rapidly, and then the CBZ contacts the medium with a high surface area to achieve a rapid dissolution effect.

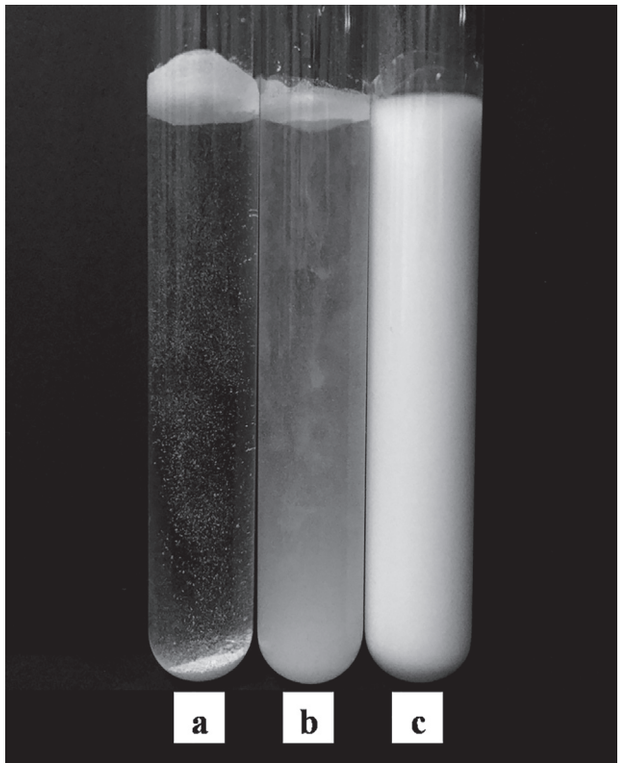

Fig. 5: The photograph of CBZ (a), PM (b) and SDs (c) dispersed in hydrochloric acid solution (pH 1.2).

2.3. Powder hydrophilicity observation

Wetting is the first step for a solid formulation to dissolve and the wettability of SDs may be related to improved dissolution (Lu et al. 2014). The hydrophilicity of CBZ, PM and SDs in hydrochloric acid (pH 1.2) is shown in Fig. 5. CBZ is a hydrophobic drug with poor wettability in hydrochloric acid solution (Fig. 5a). When mixed with Eudragit EPO, its wettability was slightly improved, but there was still a large amount of powder floating on the liquid surface (Fig. 5b). While SDs dispersed rapidly into hydrochloric acid to form a uniform milky white liquid (Fig. 5c), indicating that the wettability was greatly improved, which may be one of the reasons for its improved dissolution.

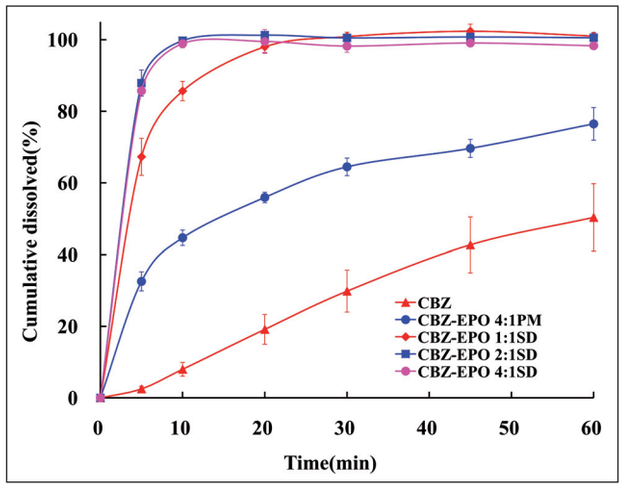

Fig. 6: Dissolution profiles of CBZ, CBZ-EPO PM and CBZ-EPO SDs with different ratios of drug:carrier (n=3).

2.4. Dissolution studies

The dissolution profiles of pure CBZ and CBZ SDs prepared with various ratios of Eudragit EPO are shown in Fig. 6. The dissolution rate of pure CBZ was very low: only 50.4 % of pure CBZ was dissolved in 60 min due to poor wettability and obvious agglomeration. After mixed with Eudragit EPO, the dissolution rate was enhanced to 76.5 % dissolved in 60 min. The HME process improved the dissolution greatly. Within the first 10 min, more than 85 % drug of all SDs samples in this study was dissolved.

Considering the crystalline form of the drug in SDs, the enhancement of CBZ dissolution rate from SDs could not be caused by the formation of polymorph I, but might be the result from the improvement of wettability, reduction of drug dispersion size and particle agglomeration. The inhibition of Eudragit EPO for the conversion of CBZ to lower solubility dihydrate in aqueous solution also improved the dissolution.

Interestingly, when the weight ratio of drug to Eudragit EPO was 4:1, the dissolution was still very fast with 85.7 % of CBZ dissolved at first 5 min, which was faster than that of SDs prepared with the ratio of 1:1. A rational reason of this phenomenon was that less polymer conduced to more fleetly exposed nanometer-sized

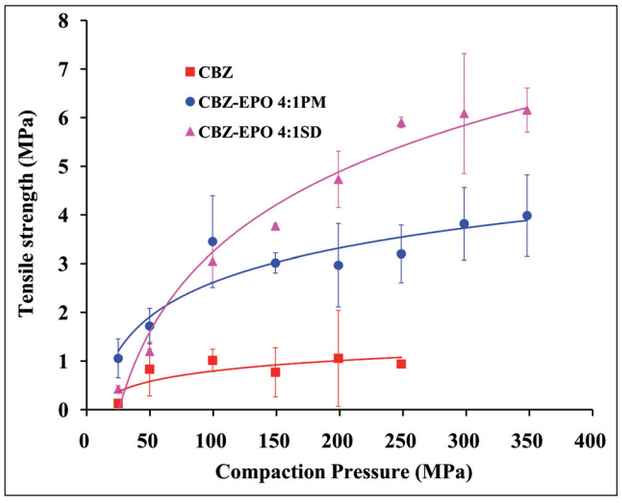

Fig. 7: Tabletability of CBZ , PM and SDs samples formulated with 20% Eudragit EPO (n = 3).

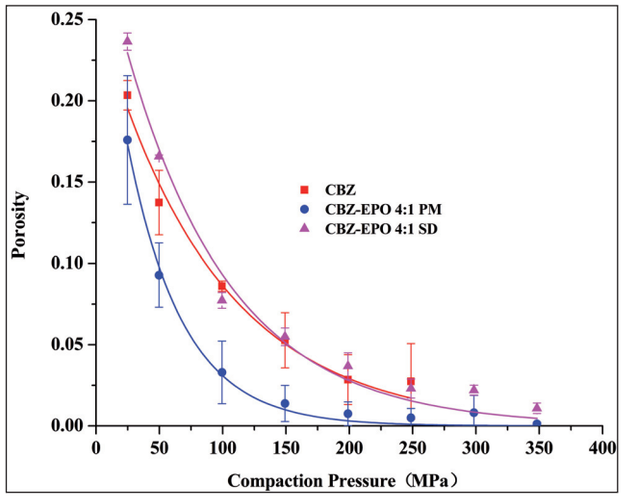

Fig. 8: Compressibility of CBZ, PM and SDs samples formulated with 20% Eudragit EPO (n = 3).

CBZ into the dissolution media. But too few polymer could not preserve the high energy state of drugs in SDs to achieve the fast dissolution. Therefore, we selected the highest drug loading SDs with drug to carrier ratio of 4:1 for further study.

2.5. *Tablet properties*

2.5.1. *Tabletability*

Tabletability describes the relationship between tensile strength of a tablet and compaction pressure exerted on these tablets (Joiris et al. 1998). Fig. 7 depicts the tabletability of tablets prepared with CBZ, PM and SDs. Pure CBZ showed a very poor tabletability with a tensile strength below 1 MPa. Increasing the compaction pressure could improve the tensile strength slightly at first, then leveled off at higher compaction pressure. When the compaction pressure was higher than 250 MPa, the tablets were prone to split. However, after adding Eudragit EPO, tabletability was improved significantly. The tensile strength of tablets made with PM or hot melt extrudates were much better than that of CBZ and no capping or lamination was observed under the compaction pressure from 25 MPa to 350 MPa. When the compaction pressure was higher than 100 MPa, the tablets tensile strength was enhanced to over 2 MPa, which was strong enough to resist stand various conditions like stress during delivery and storage. Compared to pure CBZ, the tensile strength of tablets made of PM was increased threefold even when the content of Eudragit EPO was 20 %. The tensile strength of tablets made of hot melt extrudates was improved further and rose to the level of about 6 MPa, which was nearly sixfold that of the untreated CBZ. So the SDs had much better tabletability than pure CBZ powder and PM.

2.5.2. *Compressibility*

The compressibility of powder describes the change in volume as a function of pressure and reveals basic information about the compression process, which is fundamental for the understanding of compactibility and tabletability. Under the applied pressure, the particles and their fragments rearranged into a closer packing structure resulting in a reduction of volume and increased bonding area. The reduction of volume is quantified by porosity, so the compressibility is usually represented by a plot of tablet porosity against pressure. The tablet porosity is calculated according to the tablet density and the true density of its constituents. The true density of CBZ, Eudragit EPO, their PM and SDs was determined with a helium pycnometer and the results were shown in Table 1, from which we could see that the true density of SDs was much lower than that of PM. This maybe result from the crystal form of CBZ in SDs, which was different to that in PM, as different polymorphs have different true density.

Table l: True density of CBZ, Eudragit EPO, their PM and SDs

CBZ	Eudragit EPO	PM	SDs
1.338g cm^{-3}	1.125 g cm^{-3}	1.295 g cm^{-3}	1.273 g cm^{-3}

The compressibility of pure CBZ, PM and SDs is shown in Fig. 8. With the increase in compaction pressure, the porosity decreased exponentially, which followed Heckel equation very well (Table 2). Under all the compaction pressure, the porosity of tablets made with PM was lower than that of CBZ, suggesting mixing with Eudragit EPO could improve the compressibility of CBZ. This may result from Eudragit EPO which may easily fill the pores between CBZ particles. It is very interesting that the porosity of tablets made of PM was much lower than that of SDs with the same compaction pressure applied. However, in most reported cases, the porosity of the hot-melt extruded powder was reduced compared to the mixtures (Boersen et al. 2014; Jain et al. 2014). This was caused by the microstructure of SDs, which were agglomerated by nanometer-sized particles filled with pores (Fig. 4d), while the PM granules were highly dense. This was the reason of the higher porosity of tablets made of SDs than that of CBZ under the compaction pressure below 150 MPa, too. But when the pressure was higher than 150 MPa, the SDs showed better compressibility. This was attributed to the SDs possessing lower yield strength than CBZ, which could be concluded from the parameter b in the Heckel equation (Table 2).

Table 2: Fitting results of Heckel equation in various samples

	ε_0		b(MPa^{-1})		Statistics
	Value	Error	Value	Error	Adj.R-Square
CBZ	0.2562	0.01391	0.01088	0.00090	0.9838
PM	0.3074	0.01713	0.02298	0.00150	0.9936
SD	0.3098	0.01793	0.01204	0.00102	0.9823

2.5.3. *Compactibility*

As shown in Figs. 7 and Fig. 8, the HME process deteriorated the compressibility, but the tabletability was improved significantly, which was because of the enhanced interaction force after HME. This interaction force was also described as bonding strength in the bonding area-bonding strength (BABS) model, which is a useful tool to explain the complex powder tableting behaviour (Sun 2011). Bonding strength can be quantified using compactibility. If two particles have identical size and shape, tablets at the same porosity have the same bonding area. Therefore, differences in tensile strength of two materials can be traced back to bonding

strength. Compactibility describes the relationship between tensile strength and porosity; the compactibility of CBZ, PM and SDs is shown in Fig. 9. Owing to the poor compressibility of CBZ and the capping at high pressures, different porosity ranges were obtained for CBZ and others. At any given porosity, the SDs showed higher tensile strength than that of CBZ and the PM.

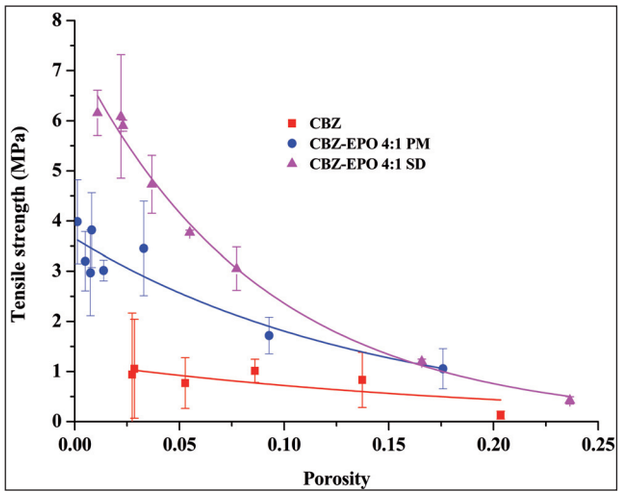

Fig. 9: Compactability of CBZ, PM and SDs samples formulated with 20% Eudragit EPO (n = 3).

From Fig. 9 we could also see the tablet tensile strength decreasing exponentially with increased porosity, which fitted the Ryshkewitch equation where T_{S0} is the extrapolated tensile strength at zero porosity. T_{S0} is often used to compare the bonding strength. The T_{S0} of pure CBZ was only 1.2 MPa, so the bonding strength of pure CBZ was poor. After mixing with one forth weight of Eudragit, the bonding strength was enhanced with the TS_0 of 3.7 MPa. The TS_0 of the SDs was enhanced to 7.4 MPa, illustrating the HME process could improve the bonding strength significantly. This may be caused by the more uniformity and closer contact during melt and extrusion. It may be also the result from the transformation of polymorphs.

3. Experimental

3.1. Materials

CBZ was purchased from Zhejiang Jiuzhou Pharmaceutical Co., Ltd (Zhejiang, China). Eudragit EPO was donated by Evonik Industries AG (Darmstadt, Germany). All other reagents were of analytical grade and used without further purification.

3.2. Preparation of SDs

CBZ SDs were processed *via* HME in various drug to carrier weight ratios using a co-rotating, fully intermeshing twin screw Minilab CTW hot melt extruder (Thermo Fisher Scientific, Longborough, Germany) operating at a screw-speed of 30 rpm and a process temperature of 140 °C across the entire barrel. The extrudates were cooled at room temperature, milled and sieved through a 120 mesh sieve.

3.3. CBZ SDs characterization

3.3.1. PXRD

The crystallinity of Eudragit EPO, CBZ, PM and SDs was determined by means of a X-ray generator (X'Pert PRO, PNAlytical, Netherlands). The Patterns were obtained using a step width of 0.03° with a detector resolution in 2θ between 3 and 35° at ambient temperature.

3.3.2. DSC

Thermograms of the samples were recorded on a DSC1/700 (Mettler-Toledo, Zurich, Switzerland). Samples (approx. 5 mg) were weighed into aluminum pans and heated from 25 to 210 °C at a heating rate of 10 °C min^{-1} under a nitrogen purge gas flow of 50 mL min^{-1}.

3.3.3. FTIR

FTIR spectra of Eudragit EPO, CBZ, PM and SDs were obtained by a Avatar370 FTIR spectrometer (Nicolet 6700, Thermo Fisher Scientific, USA) using the KBr pellet technique. For each spectrum, 32 scans were performed in the range of 4000 cm^{-1}-400 cm^{-1} with a resolution of 4 cm^{-1}.

3.4. SEM

Electron micrographs of PM and SDs were obtained by a field emission scanning electron microscope (Nano nova 450, FEI, USA) operated at an accelerating voltage of 5 kV. The samples were mounted on a metal stub with double-sided electrically conductive adhesive tape and coated with gold-palladium under the vacuum.

3.5. Powder hydrophilicity study

CBZ (100 mg), PM and SDs were added in 10 mL dilute hydrochloric acid (pH 1.2) and shaken by a constant temperature oscillator (THZ-82, Changzhou Guohua Electric Appliance Co., Ltd., Changzhou, China) at 25 °C at 100 rpm for 1 min. Then powder dispersion was checked.

3.6. Powder dissolution rate

Drug dissolution from CBZ SDs with different drug to carrier ratios was determined with a USP II dissolution apparatus (Tianda Tianfa Technology Co., Ltd., Tianjin, China) at 37 °C and a paddle speed of 75 rpm using 500 mL dilute hydrochloric acid (pH 1.2) as dissolution media SDs containing 100 mg CBZ was weighed accurately and added to the dissolution after sieving through a 120 mesh sieve. Samples (10 mL) were withdrawn at 5, 10, 20, 30, 45 and 60 min and filtered through a 0.45 µm membrane filter. The drug concentrations were detected by a UV-spectrophotometer at λ = 285 nm (New Century UV-Vis spectrophotometer T6, General Analysis Beijing General Instrument Co., Ltd.). Interference of the carriers was negligible. All dissolution tests were performed in triplicates .

3.7. Preparation and evaluation of tablets

Pure CBZ powder, PM and SDs were all sieved through a 120 mesh sieve and then compressed with a universal material testing machine (Type 8801, Instron, America) at a speed of 10 mm min^{-1} using a round (8 mm diameter) flat faced tooling. Two custom-made rigid PVC blocks were used to align the punches and die to allow successful compression. The punches and die were lubricated with magnesium stearate. The tablets were made with compaction force ranging from 1.25 KN to 17.5 KN. All tablets were allowed to relax for more than 24 h.

After relaxation, diameter and thickness of the tablets were determined with vernier calipers and the weights were measured with an analytical balance. The tablet breaking force was determined using a Texture analyzer (Stable Micro System, UK) at a speed of 0.01 mm s^{-1} with a 0.05 N trigger force. The tensile strength (*Ts*) of the tablets was derived using the following equation of Fell and Newton (Fell and Newton 1968):

$$T_s = \frac{2F}{\pi \cdot D \cdot t} \quad (1)$$

where *F*, *D* and *t* are the diametral breaking force, tablet diameter and tablet thickness, respectively.

The porosity of the tablet (ε) was calculated using the following equation:

$$\varepsilon = 1 - \frac{\rho_{Tab}}{\rho_T} \quad (2)$$

where ρ_{Tab} and ρ_t are the tablet density and true density respectively. The tablet density was calculated by dividing the tablet mass by the volume of the tablet.

The true density of CBZ, Eudragit EPO, PM and SDs was determined using an AccuPyc II 1340 helium pycnometer (Micromeritics, Norcross, USA).

Tabletability was analyzed by plotting tablet tensile strength versus compaction pressure. Compressibility was analyzed by assessment of the tablet volume reduction (tablet porosity normalized by compaction pressure). The figures were fitted by Heckel equation with mathematical transformation as Eq. (3). Compactibility of pharmaceutical powders was analyzed with the Ryshkewitch Eq. (4).

$$\varepsilon = \varepsilon_0 \cdot \exp(-b \cdot P) \quad (3)$$

$$T_s = T_0 \cdot \exp(-k \cdot \varepsilon) \quad (4)$$

where is the porosity of powder when $P = 0$; b is a constant which is inversely proportional to the yield strength of materials; *Ts* and T_0 are the tablet tensile strength and limiting tablet tensile strength at zero porosity respectively and k is an empirical constant (Ryshkewitch 1953).

Conflicts of interest: None declared

References

Agrawal AM, Dudhedia MS, Patel AD, Raikes MS (2013) Characterization and performance assessment of solid dispersions prepared by hot melt extrusion and spray drying process. Int J Pharm 457: 71–81.

Al-Hamidi H, Edwards AA, Mohammad MA, Nokhodchi A (2010) To enhance dissolution rate of poorly water-soluble drugs: Glucosamine hydrochloride as a potential carrier in solid dispersion formulations. Colloids Surf B Biointerfaces 76: 170-178.

Alam MA, Al-Jenoobi FI, Al-Mohizea AM, Ali R (2015) Effervescence assisted fusion technique to enhance the solubility of drugs. AAPS PharmSciTech 16: 1487-1494.

Alshahrani SM, Lu W, Park JB, Morott JT, Alsulays BB, Majumdar S, Langley N, Kolter K, Gryczke A, Repka MA (2015) Stability-enhanced hot-melt extruded amorphous solid dispersions via combinations of Soluplus® and HPMCAS-HF. AAPS PharmSciTech 6: 824-834.

Bhardwaj V, Trasi NS, Zemlyanov DY, Taylor LS (2018) Surface area normalized dissolution to study differences in itraconazole-copovidone solid dispersions prepared by spray-drying and hot melt extrusion. Int J Pharm 540: 106-119.

Boersen N, Lee TW, Shen XG, Hui HW (2014) A preliminary assessment of the impact of hot-melt extrusion on the physico-mechanical properties of a tablet. Drug Dev Ind Pharm 40: 1386-1394.

Chen Y, Wang S, Wang S, Liu C, Su C, Hageman M, Hussain M, Haskell R, Stefanski K, Qian F (2016) Initial drug dissolution from amorphous solid dispersions controlled by polymer dissolution and drug-polymer interaction. Pharm Res 33: 2445-2458.

Deng J, Staufenbiel S, Bodmeier R (2017) Evaluation of a biphasic in vitro dissolution test for estimating the bioavailability of carbamazepine polymorphic forms. Eur J Pharm Sci 105: 64-70.

Dinunzio JC, Schilling SU, Coney AW, Hughey JR, Kaneko N, McGinity JW (2012) Use of highly compressible Ceolus microcrystalline cellulose for improved dosage form properties containing a hydrophilic solid dispersion. Drug Dev Ind Pharm 38: 180-189.

Djuris J, Nikolakakis I, Ibric S, Djuric Z, Kachrimanis K (2013) Preparation of carbamazepine-Soluplus solid dispersions by hot-melt extrusion, and prediction of drug-polymer miscibility by thermodynamic model fitting. Eur J Pharm Biopharm 84: 228-237.

Dos Santos KM, Barbosa RM, Vargas FGA, de Azevedo EP, Lins ACDS, Camara CA, Aragão CFS, Moura TFLE, Raffin FN (2017) Development of solid dispersions of β-lapachone in PEG and PVP by solvent evaporation method. Drug Dev Ind Pharm 44: 750-756.

Douroumis D, Bouropoulos N, Fahr A (2007) Physicochemical characterization of solid dispersions of three antiepileptic drugs prepared by solvent evaporation method. J Pharm Pharmacol 59: 645-653.

Edueng K, Mahlin D, Larsson P, Bergstrom CAS (2017) Mechanism-based selection of stabilization strategy for amorphous formulations: Insights into crystallization pathways. J Control Release 256: 193-202.

Fell JT, Newton JM (1968) The tensile strength of lactose tablets. J Pharm Pharmacol 20: 657-659.

Grymonpre W, De Jaeghere W, Peeters E, Adriaensens P, Remon JP, Vervaet C (2016) The impact of hot-melt extrusion on the tableting behaviour of polyvinyl alcohol. Int J Pharm 498: 254-262.

Grzesiak AL, Lang M, Kim K, Matzger AJ (2003) Comparison of the four Anhydrous polymorphs of carbamazepine and the crystal structure of form I. J Pharm Sci. 92: 2260-2271.

Gupta SS, Parikh T, Meena AK, Mahajan N, Vitez I, Serajuddin ATM (2015) Effect of carbamazepine on viscoelastic properties and hot melt extrudability of Soluplus®. Int J Pharm 478: 232-239.

Huang S, O'Donnell KP, Keen JM, Rickard MA, McGinity JW, Williams RO 3rd (2016) A new extrudable form of hypromellose: AFFINISOL HPMC HME. AAPS PharmSciTech 17: 106-119.

Jain H, Khomane KS, Bansal AK (2014) Implication of microstructure on the mechanical behaviour of an aspirin-paracetamol eutectic mixture. CrystEngComm 16: 8471-8478.

Joiris E, Di Martino P, Berneron C, Guyot-Hermann AM, Guyot JC (1998) Compression behavior of orthorhombic paracetamol. Pharm Res 15: 1122-1130.

Kawabata Y, Wada K, Nakatani M, Yamada S, Onoue S (2011) Formulation design for poorly water-soluble drugs based on biopharmaceutics classification system: basic approaches and practical applications. Int J Pharm 420: 1-10.

Kobayashi Y, Ito S, Itai S, Yamamoto K (2000) Physicochemical properties and bioavailability of carbamazepine polymorphs and dihydrate. Int J Pharm 193: 137-146.

Kovacević I, Parojcić J, Homsek I, Tubić-Grozdanis M, Langguth P (2009) Justification of biowaiver for carbamazepine, a low soluble high permeable compound, in solid dosage forms based on IVIVC and gastrointestinal simulation. Mol Pharm 6: 40-47.

Kulkarni C, Kelly AL, Gough T, Jadhav V, Singh KK, Paradkar A (2017) Application of hot melt extrusion for improving bioavailability of artemisinin a thermolabile drug. Drug Dev Ind Pharm 44: 206-214.

Liu X, Lu M, Guo Z, Huang L, Feng X, Wu C (2012) Improving the chemical stability of amorphous solid dispersion with cocrystal technique by hot melt Extrusion. Pharm Res 29: 806-817.

Lu Y, Tang N, Lian R, Qi J, Wu W (2014) Understanding the relationship between wettability and dissolution of solid dispersion. Int J Pharm 465: 25-31.

Ma Y, Yang Y, Xie J, Xu J, Yue P, Yang M (2018) Novel nanocrystal-based solid dispersion with high drug loading, enhanced dissolution, and bioavailability of andrographolide. Int J Nanomedicine 13: 3763-3779.

Medarević DP, Kachrimanis K, Mitrić M, Djuriš J, Djurić Z, Ibrić S (2015) Dissolution rate enhancement and physicochemical characterization of carbamazepine-poloxamer solid dispersions. Pharm Dev Technol 21: 268-276.

Mohammed NN, Majumdar S, Singh A, Deng W, Murthy NS, Pinto E, Tewari D, Durig T, Repka MA (2012) Klucel EF and ELF polymers for immediate-release oral dosage forms prepared by melt extrusion technology. AAPS PharmSciTech 13: 1158-1169.

Ndindayino F, Henrist D, Kiekens F, Van den Mooter G, Vervaet C, Remon JP (2002) Direct compression properties of melt-extruded isomalt. Int J Pharm 235: 149-157.

Pan-On S, Rujivipat S, Ounaroon A, Tiyaboonchai W (2017) Development and characterization of clay facial mask containing turmeric extract solid dispersion. Drug Dev Ind Pharm 44: 590-597.

Patil S, Xalxo K, Mahadik K (2017) Probing influence of solvent on polymorphic transformation of carbamazepine using electrospray technology. J Pharm Innov 12: 309-318.

Rustichelli C, Gamberini G, Ferioli V, Gamberini MC, Ficarra R, Tommasini S (2000) Solid-state study of polymorphic drugs: carbamazepine. J Pharm Biomed Anal 23: 41-54.

Ryshkewitch E (1953) Compression strength of porous sintered alumina and zirconia. J Am Ceram Soc 36: 65–68.

Sekiguchi K, Obi N, Ueda Y (1964) Studies on absorption of eutectic mixture II. Absorption of fused conglomerates of chloramphenicol and urea in rabbits. Chem Pharm Bull 12: 134-144.

Sethia S, Squillante E (2004) Solid dispersion of carbamazepine in PVP K30 by conventional solvent evaporation and supercritical methods. Int J Pharm 272: 1-10.

Sun CC (2011) Decoding powder tabletability: roles of particle adhesion and plasticity. J Adhes Sci Technol 25: 483-499.

Treffer D, Wahl P, Mark D, Koscher G, Roblegg E, Khinast JG (2013) Hot melt extrusion as a continuous pharmaceutical manufacturing process. Melt Extrusion. Springer New York: 363-396.

Vasconcelos T, Sarmento B, Costa P (2007) Solid dispersions as strategy to improve oral bioavailability of poor water soluble drugs. Drug Discov Today 12: 1068-1075.

Verreck G, Chun I, Peeters J, Rosenblatt J, Brewster ME (2003) Preparation and characterization of nanofibers containing amorphous drug dispersions generated by electrostatic spinning. Pharm Res 20: 810-817.

Vo CL, Park C, Lee BJ (2013) Current trends and future perspectives of solid dispersions containing poorly water-soluble drugs. Eur J Pharm Biopharm 85: 799-813.

Wang J, Ye X, Lin S, Liu H, Qiang Y, Chen H, Jiang Z, Zhang K, Duan X, Xu Y (2018) Preparation, characterization and in vitro and in vivo evaluation of a solid dispersion of naringin. Drug Dev Ind Pharm 44: 1725-1732

Ye G, Wang S, Heng PW, Chen L, Wang C (2007) Development and optimization of solid dispersion containing pellets of itraconazole prepared by high shear pelletization. Int J Pharm 337: 80-87.

Yin X, Daintree LS, Ding S, Ledger DM, Wang B, Zhao W, Qi J, Wu W, Han J (2015) Itraconazole solid dispersion prepared by a supercritical fluid technique: preparation, in vitro characterization, and bioavailability in beagle dogs. Drug Des Devel Ther 28: 2801-2810.